INTERNATIONAL JOURNAL FOR NUMERICAL METHODS IN FLUIDS
Int. J. Numer. Meth. Fluids 2008; **56**:1695–1704
Published online 17 July 2007 in Wiley InterScience (www.interscience.wiley.com). DOI: 10.1002/fld.1569

Decomposition methods for time-domain Maxwell's equations

Zhi-Xiang Huang*,†, Wei Sha, Xian-Liang Wu and Ming-Sheng Chen

Key Laboratory of Intelligent Computing and Signal Processing, Anhui University, Ministry of Education Hefei, Anhui 230039, People's Republic of China

SUMMARY

Decomposition methods based on split operators are proposed for numerical integration of the time-domain Maxwell's equations for the first time. The methods are obtained by splitting the Hamiltonian function of Maxwell's equations into two analytically computable exponential sub-propagators in the time direction based on different order decomposition methods, and then the equations are evaluated in the spatial direction by the staggered fourth-order finite-difference approximations. The stability and numerical dispersion analysis for different order decomposition methods are also presented. The theoretical predictions are confirmed by our numerical results. Copyright © 2007 John Wiley & Sons, Ltd.

Received 21 March 2007; Revised 12 June 2007; Accepted 13 June 2007

KEY WORDS: decomposition; split operators; Hamiltonian function; Maxwell's equations

1. INTRODUCTION

The Hamiltonian formalism has played a key role in mathematical physics and widely applied to both classical and quantum mechanics, computational fluid dynamics, molecular dynamics and astrophysics [1–5]. The fundamental theorem of Hamiltonian mechanics suggests that the time evolution of a Hamiltonian system is the evolution of the symplectic transform. Most conventional numerical algorithms such as finite-difference and finite-element methods produce poor results for Hamiltonian systems because they usually neglect essentials of the dynamics and fail to preserve the properties of the original systems. Decomposition methods have been previously introduced in the context of numerical methods for Hamiltonian systems by Forest and Ruth [6] and Yoshida [7] and have been used successfully used in a number of situations, such as certain nonlinear wave equations [8, 9]. For an introduction and a review on numerical methods for Hamiltonian systems,

*Correspondence to: Zhi-Xiang Huang, Key Laboratory of Intelligent Computing and Signal Processing, Anhui University, Ministry of Education Hefei, Anhui 230039, People's Republic of China.
†E-mail: zxhuang@ahu.edu.cn

Contract/grant sponsor: National Natural Science Foundation of China; contract/grant numbers: 60371041, 60671051

we refer to [1]. The main advantage of the decomposition methods is that for an arbitrary order in the time direction they allow constructing algorithms, which are exactly symplectic and time reversible. In this paper, we present some fundamental theorems about Hamiltonian systems and write down Maxwell's equations in the particular infinite-dimensional Hamiltonian system form, which allows their decomposition into two computable exponential sub-propagators in the temporal direction. Then, we use the staggered fourth-order space difference operators to approximate the first-order spatial derivatives in the equations. The stability and numerical dispersion analysis and some numerical results are also included in this paper.

2. DECOMPOSITION METHODS FOR AN INFINITE-HAMILTONIAN SYSTEM

Consider a bounded region Ω, we define $M = \{\mathbf{Z} = (\mathbf{p}, \mathbf{q}) | \mathbf{p}, \mathbf{q} \in \mathscr{C}^\infty(\Omega) \cap H^1(\Omega)\}$, and $F(M) = \{F(\mathbf{p}, \mathbf{q}) | F : \text{real-value functional on } M\}$ with the Poisson bracket

$$\{T, G\} = \int_\Omega \delta T \mathbf{D} \delta G \, \mathrm{d}v, \quad \mathbf{D} = \begin{pmatrix} \mathbf{0}_3 & -\mathbf{I}_3 \\ \mathbf{I}_3 & \mathbf{0}_3 \end{pmatrix} \tag{1}$$

where $\mathbf{p}$ and $\mathbf{q}$ are vector functions with three components, $T, G \in F(M)$, $\mathbf{0}_3$ and $\mathbf{I}_3$ are 3×3 zeros and identity matrix. An infinite-dimensional Hamiltonian system on M is often referred to as Hamiltonian equations of the form

$$\frac{\partial \mathbf{p}}{\partial t} = -\frac{\delta H}{\delta \mathbf{q}}(\mathbf{p}, \mathbf{q}), \quad \frac{\partial \mathbf{q}}{\partial t} = \frac{\delta H}{\delta \mathbf{p}}(\mathbf{p}, \mathbf{q}) \tag{2}$$

where $H \in F(M)$ is a Hamiltonian function, the operator $\delta / \delta \mathbf{q}$ is the functional derivative which is defined as

$$\frac{\delta H}{\delta \mathbf{q}} = \left(\frac{\delta H}{\delta q_x}, \frac{\delta H}{\delta q_y}, \frac{\delta H}{\delta q_z} \right)^{\mathrm{T}} \tag{3}$$

while $(\delta H / \delta q_\vartheta)(\vartheta = x, y, z)$ is calculated as

$$\int_\Omega \frac{\delta H}{\delta q_\vartheta} \psi \, \mathrm{d}v = \left[\frac{\mathrm{d}}{\mathrm{d}\rho} H(q_\vartheta + \rho \psi) \right] \Big|_{\rho = 0} \tag{4}$$

where ψ is a test function. With the above notions, Hamiltonian equation (2) is written as

$$\frac{\partial \mathbf{Z}}{\partial t} = \{\mathbf{Z}, H(\mathbf{Z})\} \equiv L_H \mathbf{Z} \tag{5}$$

So the formal integration of $\mathbf{Z}(t)$ from $t = 0$ to τ is given by

$$\mathbf{Z}(t) = \exp(\tau L_H) \mathbf{z}(0) \equiv \exp[\tau (L_A + L_B)] \mathbf{Z}(0) \tag{6}$$

for a Hamiltonian function $H(\mathbf{Z}) = H(\mathbf{p}, \mathbf{q}) \equiv A(\mathbf{p}) + B(\mathbf{q})$ with the operator L_H split as $L_H = L_A + L_B$. Of course, solution (6) is only formal because the exponential propagator $\exp(\tau L_H)$ cannot

DOI: 10.1002/fld

Table I. Coefficients and $\mathrm{CFL}_{\max}$ for methods of order 2–4.

Method	Coefficients $\{c_l\}$ and $\{d_l\}$	Error	$\mathrm{CFL}_{\max}$
Second-order $S(2, 2; 4)$	$c_1 = 1 - 1/2d_1, d_1 = \frac{\sqrt{2}}{2}$ $c_2 = 1/2d_1, d_2 = 1 - d_1$	$O(\triangle t)^3$	0.5603
Third-order $S(3, 3; 4)$	$c_1 = 1, d_1 = -\frac{1}{24}$ $c_2 = -\frac{2}{3}, d_2 = \frac{3}{4}$ $c_3 = \frac{2}{3}, d_3 = \frac{7}{24}$	$O(\triangle t)^4$	0.6176
Fourth-order $S(5, 4; 4)$	$c_1 = c_5 = \xi, d_1 = d_4 = (1 - 2\gamma)/2$ $c_2 = c_4 = \chi, d_2 = d_3 = \gamma$ $c_3 = 1 - 2(\xi + \chi), d_5 = 0$ $\xi = 0.178617896, \chi = -0.066264583$ $\gamma = -0.2123418311$	$O(\triangle t)^5$	0.7263

be evaluated exactly at any τ. However, we can approximate $\exp[\tau(L_A + L_B)]$ to the pth order in the product form [7]

$$\exp[\tau(L_A + L_B)] = \prod_{l=1}^{m} \exp(d_l \tau L_B) \exp(c_l \tau L_A) + O(\tau^{p+1}) \tag{7}$$

via a well-chosen set of decomposition coefficients $\{c_l\}$ and $\{d_l\}$, m and p ($m \geqslant p$) are the number of stages or iterated numbers required in every integer time step and the order of the method, respectively. In this paper, particularly, we choose the two-stage second-order, three-stage third-order and five-stage fourth-order methods with the coefficients given in [2, 3, 10], respectively. These coefficients are also given in Table I. The main advantage of the above decomposition method is that the exponential sub-propagators $\exp(\tau L_A)$ and $\exp(\tau L_B)$ are explicitly computable while (6) is only formal.

3. MAXWELL'S EQUATIONS AS AN INFINITE-HAMILTONIAN SYSTEM

In linear isotropic material, the time-domain Maxwell's equations are written as

$$\frac{\partial \mathbf{B}}{\partial t} = -\nabla \times \mathbf{E} \tag{8}$$

$$\frac{\partial \mathbf{D}}{\partial t} = \nabla \times \mathbf{H} - \mathbf{J} \tag{9}$$

$$\mathbf{D} = \varepsilon \mathbf{E}, \quad \mathbf{B} = \mu \mathbf{H} \tag{10}$$

where ε and are μ and $\mathbf{J}$ denote the permittivity, permeability and the current density, respectively. Under the Hamiltonian framework, (8) and (9) can be rewritten in the form of an

DOI: 10.1002/fld

infinite-dimensional Hamiltonian system as

$$\frac{\partial}{\partial t}\begin{pmatrix}\mathbf{B}\\ \mathbf{D}\end{pmatrix}=\begin{pmatrix}\mathbf{0}_3 & -\mathbf{I}_3\\ \mathbf{I}_3 & \mathbf{0}_3\end{pmatrix}\begin{pmatrix}\dfrac{\delta \mathbf{H}}{\mathbf{B}}\\ \dfrac{\delta \mathbf{H}}{\mathbf{D}}\end{pmatrix} \tag{11}$$

with a suitable Hamiltonian function H given by

$$H(\mathbf{B},\mathbf{D})=\frac{1}{2}\left(\frac{1}{\mu}\mathbf{B}\cdot\nabla\times\mathbf{B}+\frac{1}{\varepsilon}\mathbf{D}\cdot\nabla\times\mathbf{D}\right)-\mathbf{J}\cdot\mathbf{B} \tag{12}$$

4. DECOMPOSITION METHODS FOR TIME-DOMAIN MAXWELL'S EQUATIONS

In this section, we will construct and present decomposition methods for Maxwell's equations. We can treat Maxwell's equations as special infinite-dimensional Hamiltonian systems with $\mathbf{p}=\mathbf{B}$ and $\mathbf{q}=\mathbf{D}$. Our methods consist of the following two steps: In step 1, we use (7) to approximate (11) in the temporal direction on the discretized time grids $\{n\Delta t, n=1,2,\ldots\}$ and every Δt-step is split into m sub-steps according to (7). During this step, the exponential sub-propagators $\exp(\tau L_A)$and $\exp(\tau L_B)$ are explicitly computable, as can be seen in the following section. In step 2, we fully discretize the first-order spatial derivatives in the three-dimensional curl operator with the staggered spatial grids $\{(i\Delta x, j\Delta y, k\Delta z)|i,j,k=\ldots,-\frac{1}{2},0,\frac{1}{2},\ldots\}$.

4.1. Discretization in the temporal domain

With some mathematical manipulation, sourceless medium (11) can be rewritten as

$$\frac{\partial}{\partial t}\begin{pmatrix}\mathbf{B}\\ \mathbf{D}\end{pmatrix}=\begin{pmatrix}\mathbf{0}_3 & -\varepsilon^{-1}\mathbf{R}\\ \mu^{-1}\mathbf{R} & \mathbf{0}_3\end{pmatrix}\begin{pmatrix}\mathbf{B}\\ \mathbf{D}\end{pmatrix}\equiv(L_A+L_B)\begin{pmatrix}\mathbf{B}\\ \mathbf{D}\end{pmatrix} \tag{13}$$

$$L_A=\begin{pmatrix}\mathbf{0}_3 & -\varepsilon^{-1}\mathbf{R}\\ \mathbf{0}_3 & \mathbf{0}_3\end{pmatrix},\quad L_B=\begin{pmatrix}\mathbf{0}_3 & \mathbf{0}_3\\ \mu^{-1}\mathbf{R} & \mathbf{0}_3\end{pmatrix} \tag{14}$$

$$\mathbf{R}=\begin{pmatrix}0 & -\dfrac{\partial}{\partial z} & \dfrac{\partial}{\partial y}\\ \dfrac{\partial}{\partial z} & 0 & -\dfrac{\partial}{\partial x}\\ -\dfrac{\partial}{\partial y} & \dfrac{\partial}{\partial x} & 0\end{pmatrix} \tag{15}$$

Since $L_\upsilon^\kappa=0$, ($\upsilon=A$ or B, $\kappa=2,3,\ldots$), the exponential operator $\exp(\tau L_A)$ and $\exp(\tau L_B)$ can be analytically computed as follows:

$$\exp(\tau L_A)=\mathbf{I}_6+\tau L_A \tag{16}$$

$$\exp(\tau L_B)=\mathbf{I}_6+\tau L_B \tag{17}$$

DOI: 10.1002/fld

Therefore, the pth-order decomposition method is applicable to the numerical integration of Maxwell's equations (13) in the temporal domain as

$$\begin{pmatrix}\mathbf{B}\\ \mathbf{D}\end{pmatrix}(\tau)=\prod_{l=1}^{m}(\mathbf{I}_6+d_l\tau L_B)(\mathbf{I}_6+c_l\tau L_A)\begin{pmatrix}\mathbf{B}\\ \mathbf{D}\end{pmatrix}(0) \tag{18}$$

4.2. Discretization in the spatial domain

Maxwell's equations need to be further discretized in the spatial direction. Here, we use finite difference to approximate the spatial derivatives. Let $f^n_{i,j,k}=f(i\Delta x, j\Delta y, k\Delta z; n\Delta t)$ approximate the exact solution $f(x, y, z)$ at point $(i\Delta x, j\Delta y, k\Delta z)$ in the nth time step. The following staggered fourth-order space difference operators are used to approximate $\partial_x f^n_{i,j,k}$:

$$LS_i\cdot f^n_{i,j,k}\equiv\frac{27(f^n_{i+\frac{1}{2},j,k}-f^n_{i-\frac{1}{2},j,k})-f^n_{i+\frac{3}{2},j,k}+f^n_{i-\frac{3}{2},j,k}}{24\Delta x}\approx\partial_x f^n_{i,j,k}+O(\Delta x^4) \tag{19}$$

If we combine the m stage p-order decomposition method with fourth-order space difference approximation, the proposed method, referred to as $S(m, p; 4)$ method, can be obtained. The detailed expressions of $\mathbf{B}$ and $\mathbf{D}$, take B_x and D_x components at the sth stage for example, in the $S(m, p; 4)$ method are as follows:

$$\begin{aligned}D_x^{n+s/p}(i+\tfrac{1}{2}, j, k)=D_x^{n+(s-1)/p}(i+\tfrac{1}{2}, j, k)+\frac{\Delta t d_l}{\mu}[&LS_j\cdot B_z^{n+(s-1)/p}(i+\tfrac{1}{2}, j, k)\\ &-LS_k\cdot B_y^{n+(s-1)/p}(i+\tfrac{1}{2}, j, k)]\end{aligned} \tag{20}$$

$$\begin{aligned}B_x^{n+s/p}(i, j+\tfrac{1}{2}, k+\tfrac{1}{2})=B_x^{n+(s-1)/p}(i, j+\tfrac{1}{2}, k+\tfrac{1}{2})&\\ +\frac{\Delta t c_l}{\varepsilon}[LS_k\cdot D_y^{n+(s-1)/p}(i, j+\tfrac{1}{2}, k+\tfrac{1}{2})&\\ -LS_j\cdot D_z^{n+(s-1)/p}(i, j+\tfrac{1}{2}, k+\tfrac{1}{2})]&\end{aligned} \tag{21}$$

where ε is the local permittivity at point $(i, j+\frac{1}{2}, k+\frac{1}{2})$.

4.3. Stability analysis of the decomposition methods

Here we will investigate the stability of the proposed $S(m, p; 4)$ method by means of the von Neumann approach, following a methodology found in [11]. For the method to be stable, we get the following condition $|\xi|\leqslant 1$. The ξ can be written as

$$\xi=1+\frac{1}{2}\sum_{l=1}^{m}g_l\left\{\frac{1}{\mu\varepsilon}\Delta t^2(\eta_x^2+\eta_y^2+\eta_z^2)\right\}^l \tag{22}$$

$$g_l=\sum_{1\leqslant i_1\leqslant j_1<i_2\leqslant j_2<\cdots<i_l\leqslant j_l\leqslant m}c_{i_1}d_{j_1}c_{i_2}d_{j_2}\ldots c_{i_l}d_{j_l}$$

DOI: 10.1002/fld

$$+\sum_{1\leqslant i_1<j_1\leqslant i_2<j_2\leqslant\cdots\leqslant i_l<j_l\leqslant m} d_{i_1}c_{j_1}d_{i_2}c_{j_2}\ldots d_{i_l}c_{j_l} \tag{23}$$

$$\eta_x=\frac{27(\mathrm{e}^{-\mathrm{j}_0k_x\Delta x/2}-\mathrm{e}^{\mathrm{j}_0k_x\Delta x/2})-(\mathrm{e}^{-\mathrm{j}_03k_x\Delta x/2}-\mathrm{e}^{\mathrm{j}_03k_x\Delta x/2})}{24\Delta x} \tag{24}$$

$$\eta_y=\frac{27(\mathrm{e}^{-\mathrm{j}_0k_y\Delta y/2}-\mathrm{e}^{\mathrm{j}_0k_y\Delta y/2})-(\mathrm{e}^{-\mathrm{j}_03k_y\Delta y/2}-\mathrm{e}^{\mathrm{j}_03k_y\Delta y/2})}{24\Delta y} \tag{25}$$

$$\eta_z=\frac{27(\mathrm{e}^{-\mathrm{j}_0k_z\Delta z/2}-\mathrm{e}^{\mathrm{j}_0k_z\Delta z/2})-(\mathrm{e}^{-\mathrm{j}_03k_z\Delta z/2}-\mathrm{e}^{\mathrm{j}_03k_z\Delta z/2})}{24\Delta z} \tag{26}$$

$$k_x=k\sin\theta\cos\phi,\quad k_y=k\sin\theta\sin\phi,\quad k_z=k\cos\theta \tag{27}$$

where k is the numerical wave number, $\mathrm{j}_0=\sqrt{-1}$, ϕ the spherical coordinates and θ the direction of wave propagation, respectively. The expression of the numerical dispersion can be found as

$$\cos(\omega\Delta t)=\xi \tag{28}$$

where ω is the radian frequency. In our numerical simulations, we use space discretization grids $\Delta x=\Delta y=\Delta z=\Delta$ and define

$$\mathrm{CFL}=\frac{\Delta t}{\Delta\sqrt{\varepsilon\mu}} \tag{29}$$

The stability of the method is determined by the maximum of CFL, i.e. $\mathrm{CFL}_{\max}$. The numerical results for $\mathrm{CFL}_{\max}$ are also given in Table I. As given in Table I, the $\mathrm{CFL}_{\max}$ becomes larger with the improved stage and order in the decomposition methods, but this is not always the case. According to our numerical analysis, the four-stage fourth-order method proposed by Forest and Ruth [6] has the worst $\mathrm{CFL}_{\max}$, which is equal to 0.3894. Thus, the method cannot be used for numerical integration of Maxwell's equations in practice. We also plot the relative phase error for $S(m, p; 4)$ method in Figure 1 at $\mathrm{CFL}_{\max}$. Of all the methods, $S(5, 4; 4)$ has lesser dispersion than $S(2, 2; 4)$ and $S(3, 3; 4)$ methods. Thus, $S(5, 4; 4)$ method permits a coarser discretization than the other methods for a given error bound.

5. NUMERICAL RESULTS

In this section, we considered a computational domain of $46\times46\times46$ grids surrounded by 10-grid perfectly matched layers (PMLs) [12] absorbing boundary conditions. A vertical dipole $P(t)$ was located near the center of the domain, at D_z point $(24, 24, 24+1/2)$. The electric dipole $P(t)$ was implemented in the $S(m, p; 4)$ method as

$$D_z^{n+s/p}(24,24,24+1/2)=D_z^{n+(s-1)/p}(24,24,24+1/2)+\frac{d_l\Delta t}{\mu}[\nabla\times\mathbf{B}]_z^{n+(s-1)/p}$$
$$-\frac{d_l\Delta t}{\mu\Delta^3}\times\frac{\mathrm{d}P(t)}{\mathrm{d}t}\bigg|_{t=(n+\sum_{l=1}^{s}c_l)\Delta t} \tag{30}$$

DOI: 10.1002/fld

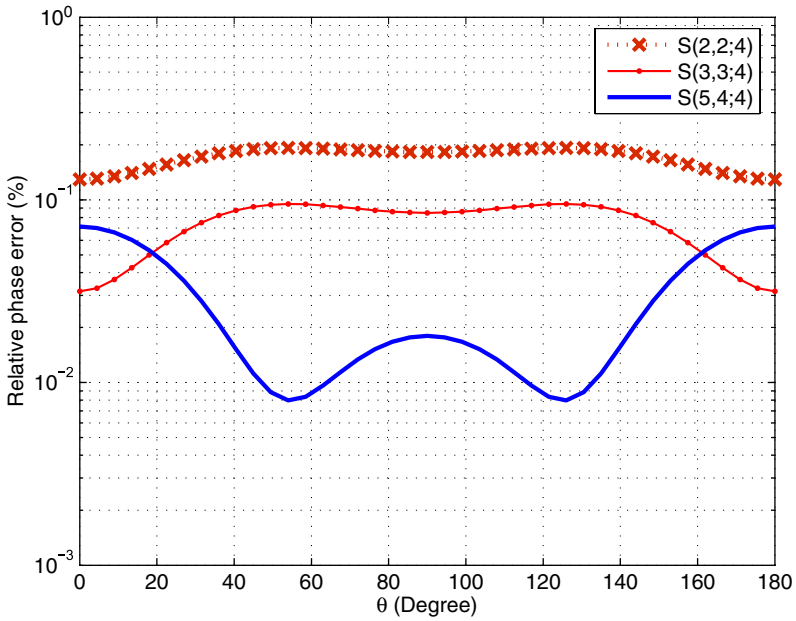

Figure 1. Dispersion curves for $S(m, p; 4)$ method at $\phi = 45°$.

The electric dipole $P(t)$ was expressed using the Gaussian pulse

$$P(t) = 10^{-10} \exp\left(-\left(\frac{t - 3T_0}{T_0}\right)^2\right) (T_0 = 2\,\text{ns}) \tag{31}$$

Figure 2 shows the values of the vertical electric field calculated by different order methods at point $(12, 22, 12 + 1/2)$, located 10 grids from the dipole and two grids from the PML, against the iteration time step. The sizes of the grids were $5 \times 5 \times 5\,\text{cm}^3$ and the CFL is equal to 0.5. The figure shows that the results computed by $S(m, p; 4)$ methods are in very good agreement with the analytical solution.

In Figure 3, we plot the error, which means the absolute difference between the values calculated by each method and the analytical solution, against the iteration time step. The mean errors are 0.0058, 0.0049 and 0.0019 for second, third and fourth orders, respectively. These results clearly show $S(5, 4; 4)$ method acquires the best accuracy, while $S(3, 3; 4)$ method acquires slightly better accuracy than $S(2, 2; 4)$ method for the same computational conditions.

In our next simulations, we use different CFLs, time steps and spatial steps for different order methods. We find that the second-order method becomes unstable, when we choose CFL = 0.6. This confirms the results of our stability analysis. The results for all the calculations are summarized in Table II.

Again, note that for roughly the same computational cost, the fourth-order method gives results that are more accurate than the second and the third-order methods, and proves to be a promising method, with advantages of high accuracy, low computational resources, the facility of large domain and long time simulation.

DOI: 10.1002/fld

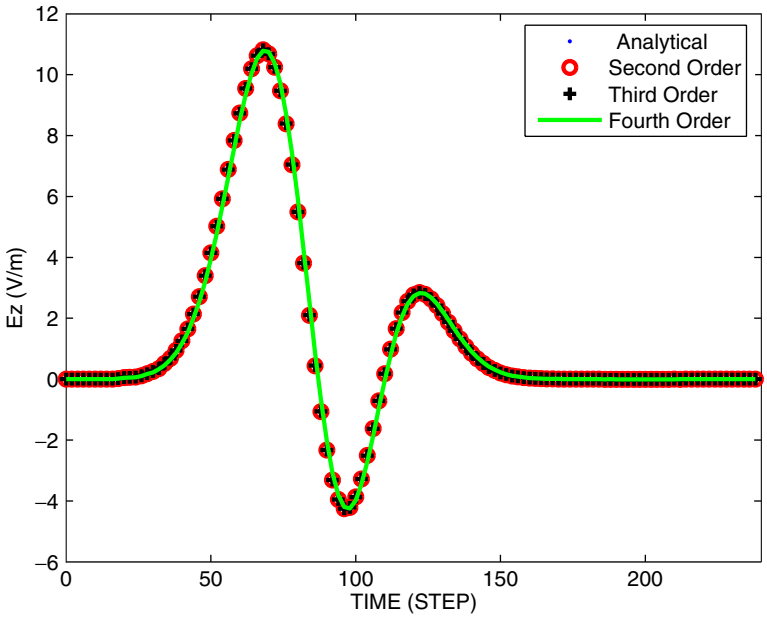

Figure 2. Electric field Ez as a function of iteration time step.

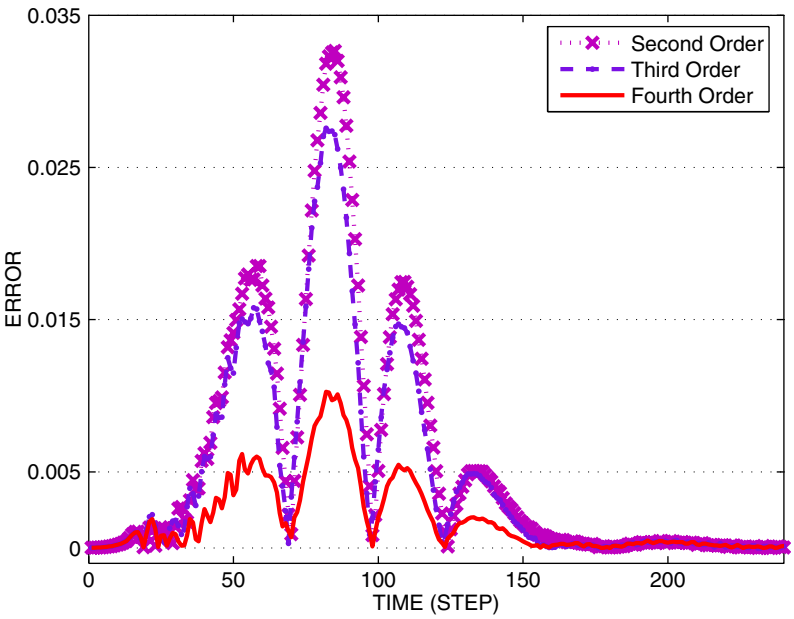

Figure 3. Error as a function of iteration time step.

DOI: 10.1002/fld

Table II. Comparison of results for different order methods.

	Second-order $S(2, 2; 4)$	Third-order $S(3, 3; 4)$	Fourth-order $S(5, 4; 4)$
Physical time	200 ns	200 ns	200 ns
CFL	0.5	0.6	0.6
Time step	83.33 ps	200 ps	200 ps
Spatial step	0.05 m	0.10 m	0.10 m
Number of steps	2400	1000	1000
Total run time	184 s	104 s	131 s
Average CPU time/step	0.0767 s	0.1040 s	0.1310 s
Error	1.5920	1.2699	0.5107

6. CONCLUSIONS

We construct a set of different order decomposition methods, denoted as $S(m, p; 4)$ methods, for approximating the solution to Maxwell's equations. The fundamental theorem and discretized strategies are also included. The stability analysis, relative phase error and the numerical results are also presented for $S(m, p; 4)$ methods. Of all the methods, the $S(5, 4; 4)$ method proves to be the most efficient method in our numerical simulations. It should be noted that the $S(2, 2; 4)$ method is identical to the high-order finite-difference time-domain method (FDTD(2, 4)) in [11] with $c_1 = 1/2$, $c_2 = 1/2$, $d_1 = 1$, $d_2 = 0$, but our second-order method acquires 13% larger $\mathrm{CFL}_{\max}$ than FDTD(2, 4) in [11], of course the second-order method can be further reduced to the traditional FDTD method [11] when a staggered second-order difference approximation is adopted to approximate the first-order spatial derivatives in the three-dimensional curl operator.

The issues of conservation of helicity, kinetic energy and vorticity by conventional Navier–Stokes solvers have been called upon to be questioned multiple times in the recent past. We hope the symplectic integration methods and split operator methods described in this paper may emerge as the solution to such problems.

ACKNOWLEDGEMENTS

The authors wish to thank the anonymous reviewers and the associate editor for their useful comments and constructive suggestions. This work was supported in part by the National Natural Science Foundation of China (Nos. 60371041 and 60671051).

REFERENCES

1. Sanz-Serna JM, Calvo MP. *Numerical Hamiltonian Problems*. Chapman & Hall: London, U.K., 1994.
2. Kostas T, Simos TE. Symplectic methods for the numerical solution of the radial Shrödinger equation. *Journal of Chemical Physics* 2002; **34**:83–93.
3. Omelyan IP, Mryglod IM, Folk R. Optimized Forest–Ruth- and Suzuki-like algorithms for integration of motion in many-body systems. *Computer Physics Communications* 2002; **146**:188–202.
4. Tanaka N, Kitayama T. Symplectic semi-Lagrangian schemes for computational fluid dynamics. *International Journal of Computational Fluid Dynamics* 2004; **13**:527–533.
5. Huang ZX, Wu XL. Symplectic partitioned Runge–Kutta scheme for Maxwell's equations. *International Journal of Quantum Chemistry* 2006; **106**:839–842.

DOI: 10.1002/fld

6. Forest E, Ruth RD. Fourth-order symplectic integration. *Physica D* 1990; **43**:105–117.
7. Yoshida H. Construction of higher order symplectic integrators. *Physics Letters A* 1990; **150**:262–268.
8. Fornberg B, Driscoll TA. A fast spectral algorithm for nonlinear wave equations with linear dispersion. *Journal of Computational Physics* 1999; **155**:456–467.
9. McLachlan R. Symplectic integration of Hamiltonian wave equations. *Numerische Mathematik* 1994; **66**:465–492.
10. Ruth RD. A canonical integration technique. *IEEE Transactions on Nuclear Science* 1983; **30**:2669–2671.
11. Taflove A, Hagness SC. *Computational Electrodynamics*: *The Finite-difference Time-domain Method*. Artech House: Boston, London, 2000.
12. Berenger JP. Three-dimensional perfectly matched layer for the absorption of electromagnetic waves. *Journal of Computational Physics* 1996; **127**:363–379.

DOI: 10.1002/fld